HHS Public Access

Dynamics of gut-brain communication underlying hunger

Lisa R. Beutler[*,2,3], **Yiming Chen**[*,3,4], **Jamie S. Ahn**[1,3], **Yen-Chu Lin**[1,3], **Rachel A. Essner**[1,3], and **Zachary A. Knight**[1,3,4]

[1]Department of Physiology, University of California, San Francisco, San Francisco, CA 94158

[2]Department of Medicine, University of California, San Francisco, San Francisco, CA 94158

[3]Kavli Center for Fundamental Neuroscience, University of California, San Francisco, San Francisco, CA 94158

[4]Neuroscience Graduate Program, University of California, San Francisco, San Francisco, CA 94158

Summary

Communication between the gut and brain is critical for homeostasis, but how this communication is represented in the dynamics of feeding circuits is unknown. Here we describe nutritional regulation of key neurons that control hunger *in vivo*. We show that intragastric nutrient infusion rapidly and durably inhibits hunger-promoting AgRP neurons in awake, behaving mice. This inhibition is proportional to the number of calories infused but surprisingly independent of macronutrient identity or nutritional state. We show that three gastrointestinal signals – serotonin, CCK, and PYY – are necessary or sufficient for these effects. In contrast, the hormone leptin has no acute effect on dynamics of these circuits or their sensory regulation, but instead induces a slow modulation that develops over hours and is required for inhibition of feeding. These findings reveal how layers of visceral signals operating on distinct timescales converge on hypothalamic feeding circuits to generate a central representation of energy balance.

Graphical abstract

Beutler et al. reveal how nutritional signals regulate the hypothalamic hunger circuit. They show that intragastric nutrients inhibit AgRP neurons rapidly in a way dependent solely on calorie content, whereas the satiety hormone leptin only acts on timescale of hours.

Introduction

Energy homeostasis requires communication between the body and brain. This communication is mediated by a web of hormones, metabolites, and ascending neural signals that report on the nutritional state of the body (Cummings and Overduin, 2007). The targets of these signals are thought to be neurons in the hypothalamus and related structures that integrate this information in order to generate a central representation of physiologic state (Clemmensen et al., 2017). While this gut-brain communication has been studied for decades by manipulating the signals and sensors that comprise the afferent pathways (Sohn et al., 2013), we still know remarkably little about how interoception is represented in the dynamics of the target neural circuits. Indeed, it remains a mystery how even basic visceral events, such as nutrient detection in the gut, are encoded by feeding circuits in a living animal.

AgRP and POMC neurons are the two most widely-studied cell types that control feeding. AgRP neurons are activated by fasting and promote food seeking and consumption, whereas POMC neurons are inhibited by food deprivation and promote satiety (reviewed in (Andermann and Lowell, 2017)). These two sets of neurons are intermingled in the arcuate nucleus of the hypothalamus and project broadly to a common set of subcortical structures, where they have opposing effects on food intake and other autonomic and behavioral outputs modulated by energy balance.

Due to their robust regulation by nutritional state, AgRP and POMC neurons provide a unique entry point into the study of mechanisms of interoception. Traditionally, the nutritional regulation of these cells has been investigated in two ways: by using slice physiology to measure the direct effects of hormones and nutrients on these cells *in vitro* (Cowley et al., 2001; Cowley et al., 2003; Pinto et al., 2004; van den Top et al., 2004) and by using mouse genetics to perturb these nutrient-sensing pathways and then measure the effect on physiology and behavior (reviewed in (Sohn et al., 2013)). While much has been learned using these approaches, they do not provide information about neural activity *in vivo*, and consequently cannot reveal the natural dynamics of these cells or their modulation by physiologic signals that are absent from *ex vivo* preparations.

To bridge this gap, we and others recently recorded the dynamics of AgRP and POMC neurons in awake, behaving mice (Betley et al., 2015; Chen et al., 2015; Mandelblat-Cerf et al., 2015). However the unexpected finding from these studies was that AgRP and POMC neuron activity *in vivo* is dominated by external sensory cues associated with food: when a hungry mouse detects food, or conditioned cues that predict food availability, AgRP neurons become inhibited and POMC neurons become activated within seconds. As a result, the functional state of the arcuate feeding circuit is "reset" by the sensory detection of food, in a way that predicts the nutritional content of a meal before it begins. While this discovery raised a host of new questions about the neural regulation of feeding (Chen and Knight, 2016), it also complicated our ability to probe the underlying nutritional regulation of these cells, because it revealed that the direct effects of nutrients are masked by faster, anticipatory responses.

To overcome this obstacle, we have developed a protocol for recording neural dynamics while feeding mice by intragastric infusion, thereby bypassing sensory cues associated with food. We describe here the application of this approach to dissect mechanisms of gut-brain communication underlying hunger. We show that intragastric nutrients rapidly and durably inhibit AgRP neurons in a way that is proportional to the total number of calories delivered but independent of macronutrient composition or nutritional state of the animal. We further show that three satiation signals – serotonin (5HT), cholecystokinin (CCK), and peptide YY (PYY) – are necessary or sufficient for the inhibition of AgRP neurons by intragastric nutrients. In contrast, we find that the widely-studied hormone leptin only modulates AgRP and POMC neuron dynamics on a timescale of hours, and that this slow modulation is required for leptin's effects on feeding. These findings reveal for the first time how diverse nutritional inputs are integrated in the arcuate nucleus of awake mice to enable the neural control of feeding.

Results

Sustained inhibition of AgRP neurons requires food consumption

The sensory detection of food inhibits AgRP neurons within seconds, but this inhibition is transient unless the food is subsequently consumed (Betley et al., 2015; Chen et al., 2015). To illustrate this phenomenon, we analyzed the response of AgRP neurons to presentation of inaccessible food (Figure 1A). Mice were equipped for recording calcium dynamics in AgRP neurons by fiber photometry (Chen et al., 2015) and then fasted overnight. Presentation of 'caged' chocolate that mice could see and smell but not consume resulted in a rapid inhibition of AgRP neurons (F/F -20.1 ± 5.1% from baseline at 5 min; Figure 1B, C). However, despite continued presence of the caged chocolate, this inhibition was reversed within 20 minutes (F/F -7.1 ± 3.1% from baseline at 20 min; Figure 1B,C). Subsequent presentation of accessible chocolate that mice could eat resulted again in a rapid inhibition of AgRP neuron activity (F/F -28.7% ± 6.6% from baseline at 5 min), but in this case AgRP neuron inhibition was sustained for the duration of the experiment (F/F -24.9% ± 5.3% from baseline at 20 min), persisting even after the chocolate was removed (-21.7 ± 4.7% 10 min after chocolate removal Figure 1B,C). Thus food consumption is required for long-lasting inhibition of AgRP neuron activity.

Intragastric nutrients rapidly and durably inhibit AgRP neuron activity

The mechanism by which food intake stabilizes the rapid sensory inhibition of AgRP neurons is unknown. One possibility is that AgRP neurons are inhibited by an oropharyngeal signal generated during the act of eating, analogous to how thirst neurons are inhibited by the sensation of water in the oral cavity (Zimmerman et al., 2016). Alternatively, AgRP neurons could be inhibited as a consequence of nutrient detection in the gut (Tellez et al., 2013; Tolhurst et al., 2012). To distinguish between these possibilities, we equipped mice with an intragastric catheter for direct infusion of nutrients into the stomach as well as an optical fiber for photometry recordings from AgRP neurons (Figure 1D). This preparation enables direct observation AgRP neuron responses to internal nutritional changes while bypassing exterosensory and oropharyngeal cues associated with feeding.

Mice were fasted overnight and then received an intragastric infusion of different solutions while AgRP neuron dynamics were monitored by photometry. Infusion of the liquid diet Ensure caused a rapid and progressive decrease in AgRP neuron activity (F/F -14.7 ± 6.1% from baseline at 5 min, -20.2 ± 5.5% at the end of infusion; Figure 1E,F). This inhibition persisted following the end of infusion (F/F -25.2 ± 6.3% from baseline 10 min after the end of infusion; Figure 1E,F), demonstrating that intragastric nutrients can durably inhibit AgRP neuron activity. In contrast, water infusion had no effect on AgRP neuron dynamics (F/F -2.2 ± 2.5% from baseline at the end of infusion; Figure 1E,F), indicating that gastric distension is insufficient to inhibit these cells (Figure S1). These neural responses were not secondary to learning, because we observed a robust reduction of AgRP neuron activity during the first infusion of Ensure in each animal (Figure 1G, right), whereas the lack of response to water was maintained following months of intermittent testing (Figure 1G, left). Thus gastrointestinal nutrients are sufficient to rapidly and durably inhibit AgRP neuron activity.

AgRP neuron inhibition is proportional to the number of calories infused, but independent of macronutrient identity or nutritional state

Ensure is a complex mixture of sugars, fats, and protein. To determine which of these components mediates the inhibition of AgRP neurons, we measured the neural response to intragastric infusion of isovolemic and isocaloric solutions of glucose, lipid, or peptide (Figure 2A-F). Surprisingly, intragastric infusion of each of these individual macronutrients to fasted mice caused a similar reduction in AgRP neuron activity (F/F -26.5 ± 5.5% for glucose, -25.7 ± 5.0% for lipid, -16.8 ± 3.8% for peptide at the end of infusion, $P<0.01$ compared to water). These responses were sustained following the completion of infusion (Figure 2A-C), indicating that individual macronutrients are sufficient to durably reset AgRP neuron activity. To explore further the role of nutrient identity in AgRP neuron regulation, we compared the response to infusion of three additional sugars: fructose, galactose, and sucrose (Figure 2J). Remarkably, infusion of isocaloric solutions of each of these mono- and disaccharides caused a similar inhibition of AgRP neurons, whereas infusion of the non-caloric but structurally similar sweetener sucralose had no effect on AgRP neuron activity (F/F -2.1 ± 0.7% at the end of infusion; p=0.99 compared to water; Figure 2J). Thus AgRP neurons are inhibited by intragastric delivery of a broad range of nutrients, but not by chemically related, non-nutritive substances.

The observation that any macronutrient can inhibit AgRP neuron activity (Figure 2A-C) suggests that the calorie content of the infusate may be the primary determinant of the neural response. To test this possibility, we infused glucose solutions of equal volume but different concentrations (6% to 45%) into the stomach of fasted mice. This resulted in a striking dose-dependent inhibition of AgRP neuron activity (two-way ANOVA dose effect $P<10^{-3}$; Figure 2D, G). We observed a similar dose-dependent inhibition following infusion of solutions of lipid (Figure 2E, H) and protein (Figure 2F, I). Thus the degree of inhibition of AgRP neurons by intragastric nutrients is proportional to the number of calories delivered.

We next asked how the response to nutrient infusion would be modulated by changes in nutritional state. Previously, we showed that the sensory detection of food inhibits AgRP

neurons in fasted but not fed mice (Chen et al., 2015). To test whether fasting also gates the response of AgRP neurons to nutrient delivery, we infused Ensure into the stomach of fed mice while recording AgRP neuron dynamics (Figure 2K). Surprisingly, we found that AgRP neuron activity was further reduced by intragastric Ensure even in fed animals (ΔF/F -21.3 ± 7.2% in fed mice infused with Ensure versus -4.6% ± 3.6% for water, $P = 0.012$). We observed a similar reduction of AgRP neuron activity in fed mice that received intragastric glucose or lipid (Figure 2K). Thus, in contrast to their regulation by external sensory cues, AgRP neurons in fed mice can be further inhibited by delivery of intragastric nutrients. This discrepancy has implications for our understanding of how AgRP neuron activity encodes changes in energy balance.

Intragastric nutrients diminish the sensory response of AgRP neurons to subsequently presented food

We next investigated how intragastric feeding influences the response of AgRP neurons to the sensory detection of food. Animals were fasted overnight and then infused with intragastric nutrients or water. Following infusion, animals were presented with a piece of chow and the response of AgRP neurons was measured. In mice infused with water, food presentation rapidly and robustly inhibited AgRP neuron activity (Figure 3A), whereas intragastric infusion of Ensure significantly attentuated this sensory response (ΔF/F -31.6 ± 5.6% after water versus -15.6 ± 5.8% after Ensure, $P = 0.01$; Figure 3A). Infusion of isocaloric solutions of glucose, lipid, or protein each caused a similar or stronger attentuation of the sensory response (Figure 3A). This effect was dose-dependent, with infusion of increasing concentrations of glucose resulting in a progressive decrease in the inhibition of AgRP neurons by chow presentation (Figure 3C). Thus intragastric nutrients are sufficient to block the response of AgRP neurons to external sensory cues associated with food.

The inhibition of AgRP neurons by the sensory detection of food has been proposed to represent a prediction of the number of calories that will be consumed in a forthcoming meal (Chen and Knight, 2016; Chen et al., 2015). To test this idea, we measured food intake in the first 20 minutes after presentation of chow in the experiments above (Figure 3B, D), and then correlated this food intake with the prior response of AgRP neurons to the sensory detection of food (Figure 3E). This revealed a striking correlation between these two parameters: the greater the reduction in AgRP neuron activity that occurred upon food detection, the more food the mouse subsequently consumed ($R^2 = 0.36$, $P = 0.02$, Figure 3E).

To test whether this correlation between AgRP neuron sensory response and subsequent food intake extends to other conditions, we investigated the effect of treatment with lipopolysaccharide (LPS), a bacterial toxin that causes visceral malaise and inhibits food intake. We found that treatment of fasted mice with LPS significantly reduced both the inhibition of AgRP neurons by food presentation (ΔF/F -35.1 ± 4.1% after vehicle versus -13.1 ± 3.1% after LPS, $P < 10^{-4}$) and subsequent food intake (0.57 g after vehicle versus 0.10 g after LPS, $P < 10^{-4}$) (Figure S3A-C). Analysis of individual LPS-treated animals revealed a clear correlation between these two parameters: animals that consumed no food

showed essentially no sensory inhibition of AgRP neurons, whereas animals that consumed some food had a diminished but measurable response (Figure S3D). These findings further support a model in which the sensory regulation of AgRP neurons encodes a prediction of imminent food consumption (Chen and Knight, 2016; Chen et al., 2015).

The inhibition of AgRP neurons during nutrient infusion does not require changes in blood glucose

Intragastric nutrients begin to inhibit AgRP neuron activity within five minutes of the start of infusion (Figure 1E). This timing suggests that a signal triggered by nutrient detection in the gut likely mediates the inhibition of AgRP neurons, but it does not rule out a role for a change in the level of a circulating metabolite.

To distinguish between these mechanisms, we first analyzed the role of blood glucose, since glucose has been proposed to inhibit AgRP neurons directly (Becskei et al., 2008). We observed no change in blood glucose following intragastric infusion of fat or protein (Figure S2A), indicating that the inhibition of AgRP neurons by those macronutrients is glucose-independent. In contrast and as expected, intragastric infusion of glucose caused a dose-dependent rise in blood glucose measured at the completion of infusion (Figure S2B). To assess whether this rise in blood glucose was sufficient to explain the concomitant inhibition of AgRP neurons, we measured the neural response to an equivalent parenteral glucose dose. We found that intraperitoneal (IP) glucose (4.5 g/kg) caused only a transient reduction of AgRP neuron activity (F/F -10.8 ± 1.4% at 5 min versus -1.7 ± 1.8% at 30 min, Figure S2D, E). In contrast, a similar dose of glucose delivered intragastrically (12% glucose) resulted in a stronger and sustained inhibition (F/F -10.1 ± 2.1% at 5 min and -17.1 ± 5.7% at 30 min, Figure S2D,E). This was true even though animals that received IP glucose exhibited a robust increase in circulating glucose levels that persisted for at least 30 minutes (Figure S2C). Thus, changes in blood glucose levels are not correlated with the inhibition of AgRP neurons following administration of glucose or other nutrients, and therefore blood glucose cannot explain the inhibition of AgRP neurons by intragastric nutrient infusion.

The gut-secreted hormones 5HT, CCK, and PYY are sufficient for the inhibition of AgRP neurons

Nutrient detection in the gut triggers the release of many hormones that inhibit food intake (Clemmensen et al., 2017; Tolhurst et al., 2012). To investigate whether these satiation signals are able to regulate AgRP neuron activity, we fasted mice overnight, challenged them with IP injection of a panel of candidate hormones, and then measured the response by photometry.

Three gastrointestinal hormones were sufficient to reduce AgRP neuron activity following peripheral injection: 5HT, CCK, and PYY (Figure 4A-C). Among these, PYY has previously been proposed to regulate AgRP neuron activity (Acuna-Goycolea and van den Pol, 2005; Riediger et al., 2004), whereas a role for peripheral 5HT and CCK has not been described. Interestingly, these three signals showed different kinetics of AgRP neuron inhibition *in vivo* (Figure 4A-C). 5HT and CCK caused a rapid but transient reduction in AgRP neuron activity (T_{max} inhibition CCK = 186±1s, 5HT = 446±113s), whereas PYY induced a slower,

more sustained response (T_{max} inhibition 1409±196s). Since these hormones are co-released from the gut following food ingestion, we challenged fasted mice with injection of combinations of these signals. Co-injection of CCK and PYY resulted in a rapid and sustained inhibition of AgRP neurons that matched the linear superposition of the response to the individual hormones (Figure 4D; Figure S4A, D). In contrast, co-injection of CCK and 5HT had no additive effect (Figure S4B, D). The responses to individual hormones were unaffected by whether the mice were fasted or fed (Figure S4E), consistent with the ability of intragastric nutrients to reduce AgRP neuron activity even in fed animals (Figure 2K).

We observed no response of baseline AgRP neuron activity to peripheral injection of lithium chloride or LPS (Figure 4G), two agents that are commonly used to induce nausea. Thus visceral malaise is unlikely to contribute to the inhibition of AgRP neurons following administration of 5HT, CCK, or PYY. We also found that a number of hormones implicated in the control of food intake had no acute effect on AgRP neuron dynamics (Figure 4E, F), including amylin, glucagon, glucagon-like peptide-1 (GLP-1), and, surprisingly, leptin (Figure 4F, S5). Thus AgRP neurons are rapidly modulated by a subset of peripheral signals involved in energy homeostasis.

Gastrointestinal satiation signals are differentially required for the regulation of AgRP neurons

The preceding data demonstrate that peripheral 5HT, CCK, and PYY are sufficient to inhibit AgRP neurons. To test whether these hormones are necessary, we treated mice with antagonists of their receptors and then recorded AgRP neuron calcium dynamics, both at baseline and in response to infusion of specific nutrients.

CCK inhibits food intake by binding to CCK-A receptors (CCKARs) in the periphery and brain (Reidelberger, 1994). Treatment of mice with a selective CCKAR antagonist (devazepide) had no effect on the baseline activity of AgRP neurons in fasted mice (Figure 5A,D), but dramatically attenuated the lipid-mediated inhibition of AgRP neurons (F/F -35.5 ± 3.5% after vehicle + lipid versus -11.9 ± 1.7% after devazepide + lipid infusion, $P =$ <0.001, Figure 5E,G). In contrast, devazepide pretreatment had no effect on the response of AgRP neurons to intragastric glucose infusion (Figure 5F,H). This indicates that CCK is required for the inhibition of AgRP neurons by fat but not glucose, which is consistent with the observation that fat is the most potent stimulus for CCK secretion *in vivo* (Berthoud, 2008; Tolhurst et al., 2012).

Analysis of 5HT signaling is complicated by the presence of 14 different receptors. Among these, the 5HT 3A receptor (5HTR3A) is highly expressed in vagal afferents and has been implicated in nutrient sensing (Berthoud, 2008). However, we found that treatment with a 5HTR3A antagonist (ondansetron) had no effect on the baseline activity of AgRP neurons in fasted mice (Figure 5B,D) or their inhibition by intragastric lipid or glucose infusion (Figure 5I-L). Thus HTR3A signaling is individually dispensable for the regulation of AgRP neurons, but may modulate these cells in concert with other 5HT receptors.

PYY acts through NPY2 receptors (NPY2Rs) expressed in both the periphery and brain (Broberger et al., 1997). Unexpectedly, we found that treatment of fasted mice with an

NPY2R antagonist (JNJ-31020028) caused a rapid increase in the activity of AgRP neurons at baseline (F/F -5.0 ± 3.2% after vehicle versus 19.8 ± 2.3%, $P = 0.006$ Figure 5C, E). In contrast JNJ-31020028 had no effect on the inhibition of AgRP neurons by infusion of intragastric lipid or glucose (Figure 5M-P). This indicates that AgRP neurons are under tonic inhibition by an NPY2R-mediated signal in fasted mice, but that PYY is dispensable for their nutritional regulation by fat or sugar consumption.

Leptin has no acute effect on calcium dynamics in AgRP and POMC neurons measured by photometry

Leptin is a critical regulator of arcuate feeding circuits, but we observed no acute effect of leptin on AgRP neuron activity in fasted mice, either when leptin was injected alone (Figure 5F and S5) or in combination with CCK (Figure S4C). This was unexpected because leptin has been reported to rapidly inhibit AgRP neuron activity *in vitro* ((Takahashi and Cone, 2005; van den Top et al., 2004) but see also (Claret et al., 2007)) and to synergistically inhibit food intake when co-administered with CCK (Barrachina et al., 1997). We therefore investigated in more detail how leptin modulates arcuate feeding circuits *in vivo*.

We first extended our analysis to include POMC neurons, which are activated by leptin *in vitro* (Cowley et al., 2001), and also to test the role of nutritional state. We observed no acute effect of leptin administration on the dynamics of either AgRP (Figure S5A-D) or POMC neurons (Figure S5I-L) in either fasted or fed animals. To increase the sensitivity of our assay, we repeated these experiments in knockout mice that have no endogenous leptin and thus are hypersensitive to exogenous leptin (AgRP[Cre] ob/ob and POMC[Cre] ob/ob). Remarkably, we failed to observe any rapid leptin-induced change in AgRP (Figure S5E-H) or POMC neuron (Figure S5M-P) dynamics even in an ob/ob background and even after increasing the dose of leptin to supraphysiologic levels (Figure S5Q,R). We confirmed the bioactivity of our leptin by showing that it induced pSTAT3 in the arcuate nucleus after peripheral injection (Figure S5U-X), and further that it reduced food intake and body weight in ob/ob mice (Figure 6L,M and Figure 8F). We also confirmed the functionality of our photometry assay by validating that each mouse showed a robust response to two positive control stimuli: ghrelin administration to fed mice (Figure S5S, T), and food presentation to fasted mice (Figure 7). Thus, despite *in vitro* data suggesting that leptin rapidly modulates the electrical activity of AgRP and POMC neurons, we find that leptin has no acute effect on the calcium dynamics of these cells *in vivo*.

Leptin gradually inhibits AgRP neurons and activates POMC neurons on a timescale of hours

In addition to rapid modulation of ionic currents, leptin can also induce changes in gene expression that develop over hours and have long-term effects on synaptic plasticity (Pinto et al., 2004). To investigate these slower responses *in vivo*, we administered leptin by IP injection to fasted ob/ob mice as well as ob/+ littermates, and then recorded the photometry response of AgRP and POMC neurons for three hours in the absence of food (Figure 6). This revealed a slow onset activation of POMC neurons (F/F= 13.8 ± 2.3 for leptin versus -10.7 ± 2.3 for vehicle $P<0.0001$; Figure 6C, D) and inhibition of AgRP neurons (F/F= -15.0 ± 1.9 for leptin versus -3.4 ± 2.0 for vehicle, $P = 0.0018$; Figure 6H, I). As expected,

this modulatory effect was smaller in ob/+ animals that have endogenous leptin (Figure 6B,G). In fed animals leptin failed to induce any change in AgRP or POMC neuron dynamics after three hours, even in ob/ob mice (Figure 6E,J and Figure S5). Thus, leptin induces a reciprocal activation of POMC neurons and inhibition of AgRP neurons that develops on a timescale of hours, is enhanced in leptin-deficient animals, and is only evident in a state of food deprivation.

To explore further these long-term effects, we measured the neural response to leptin infusion (Figure 6K). ob/ob mice were equipped for photometry measurements of AgRP or POMC neurons and then implanted with subcutaneous mini-osmotic pumps dispensing leptin or vehicle. Following pump implantation, vehicle-treated animals were pair-fed to leptin-treated animals to eliminate any effects of differential food intake. As expected, leptin treatment caused a precipitous decrease in food intake and body weight (Figure 6L, M). Periodic photometry measurements in these mice revealed that, relative to vehicle-treated controls, leptin induced activation of POMC neurons and inhibition of AgRP neurons (Figure 6N, O). This modulation reached a maximum within three days and persisted through the termination of the experiment (F/F= -38.9 ± 6.0% for AgRP-leptin versus -2.5 ± 11.3% for AgRP-vehicle, *P*= 0.017; F/F= 4.2 ± 9.1% for POMC-leptin versus -28.8 ± 7.2% for POMC-vehicle, *P*= 0.015; Figure 6N, O). Thus chronic leptin infusion induces a durable modulation of AgRP and POMC neuron activity *in vivo*, consistent with the effects of this hormone on feeding.

Leptin is neither necessary nor sufficient for gating the sensory regulation of AgRP and POMC neurons

In addition to regulating the baseline activity of AgRP and POMC neurons, leptin could also modulate their sensitivity to other signals, including the sensory detection of food (Betley et al., 2015; Chen et al., 2015; Mandelblat-Cerf et al., 2015). We therefore investigated how leptin might alter the responsiveness of these neurons to food cues.

We first compared the neural response to food presentation in ob/ob and ob/+ mice (Figure 7). As expected, presentation of chow to fasted ob/+ mice rapidly activated POMC neurons and inhibited AgRP neurons, whereas presentation of chow to fed mice had little effect (Figure 7C, G). Unexpectedly, the response of ob/ob mice to chow presentation was also strictly dependent on nutritional state, with responses in fasted but not fed animals (F/F= 33.1 ± 6.6% for fasted versus 2.1 ± 2.6% for fed POMC, *P* = 0.0019; F/F= -17.9 ± 1.9% for fasted versus -1.9 ± 2.0 for fed AgRP, *P* = 0.0005; Figure 7B,F). We extended this analysis by measuring the neural responses to presentation of peanut butter, an energy rich food that modulates AgRP and POMC neurons even in fed animals (Chen et al., 2015). Again, the neural response of ob/ob mice to food presentation was indistinguishable from ob/+ littermates (Figure S6). Thus, although ob/ob mice are hyperphagic, the regulation of their AgRP and POMC neurons by food cues remains dependent on whether the animal is fasted or fed.

Given that leptin is not necessary for regulation of AgRP or POMC neurons by food cues (Figure 7A-H), we tested whether it is sufficient. Fasted mice were challenged with peripheral leptin injection and the neural response to chow presentation measured three

hours later. We chose this time point because three hours is required to observe robust changes in AgRP and POMC neuron activity after leptin injection (Figure 6). In animals pre-treated with leptin, we observed a trend toward reduced activation of POMC neurons (Figure 7I-L) and reduced inhibition of AgRP neurons (Figure 7M-P) in response to food presentation in both ob/ob and ob/+ genetic backgrounds. However none of these effects reached significance when compared to vehicle-treated controls (Figure 7L, P). Taken together, these data demonstrate that changes in plasma leptin concentrations across a wide range have little to no effect on the nutritional gating of the sensory regulation of AgRP and POMC neurons. Thus, other nutritional signals must play a dominant role in regulating the sensitivity of these neurons to sensory cues.

AgRP neurons are epistatic to leptin's effects on food intake

Leptin administration profoundly inhibits food intake in ob/ob mice, but the identity of the key neural targets remains unresolved (Myers et al., 2009). We therefore investigated how AgRP neuron activity functionally interacts with leptin in the control of feeding behavior (Figure 8).

To enable manipulation of AgRP neuron activity, we generated mice that express channelrhodopsin-2 (ChR2) in AgRP neurons in either wild-type (AgRP^{ChR2}) or leptin-deficient (AgRP^{ChR2} ob/ob) genetic backgrounds, and then equipped these mice with an optical fiber positioned above the arcuate nucleus (Figure 8A). In the absence of photostimulation, *ad libitum* fed mice ate little during a 60-minute trial (0.21 ± 0.04 g for wild-type versus 0.33 ± 0.05 g for ob/ob; Figure 8B-D). Stimulation of AgRP neurons for 60 minutes prior to food availability (Chen et al., 2016) resulted in a significant increase in subsequent food intake that was similar between groups (0.74 ± 0.07 g for wild-type versus 0.76 ± 0.10 g for ob/ob; two way ANOVA effect of stimulation, $P < 10^{-3}$). The striking similarity in food intake between wild-type and ob/ob mice was not due to a ceiling effect, because both genotypes consumed more food during an alternative costimulation protocol (1.24 ± 0.14 g for wild-type versus 1.07 ± 0.14 g for ob/ob). The fact that ob/ob mice do not consume more food than wild-type animals following AgRP neuron stimulation is consistent with a model in which leptin deficiency increases food intake by acting at or upstream of AgRP neuron activity.

To test this a different way, we investigated the interaction between leptin treatment and AgRP neuron stimulation. AgRP^{ChR2} ob/ob mice were treated with leptin or vehicle by continuous subcutaneous infusion (Figure 8E). Leptin treatment resulted in a significant reduction in body weight over the first three days of infusion (Figure 8F) and leptin-treated animals ate less food than vehicle-treated controls in a 60-minute trial conducted without photostimulation (0.05 ± 0.02 g for leptin-treated versus 0.32 ± 0.04 g for vehicle-treated; Figure 8G, H). However, prestimulation of AgRP neurons for 60 minutes prior to food availability resulted in increased food intake that was similar between groups (0.47 ± 0.07 g for leptin-treated versus 0.60 ± 0.08 g for vehicle-treated; Figure 8G,H). This similarity in food intake between leptin and vehicle-treated animals was again not due to a ceiling effect, because both cohorts consumed more food during a costimulation protocol (0.89 ± 0.22 g for leptin-treated versus 0.76 ± 0.15 g for vehicle-treated; Figure 8G, H). Thus AgRP neuron

photostimulation can bypass the ability of leptin to block food intake, suggesting that inhibition of AgRP neurons is required for leptin's effects on feeding.

Discussion

Feeding is regulated by communication between the gut and brain. For decades, this process has been studied by manipulating hormones and other peripheral signals and then measuring the effect on behavior (Richter, 1942). While much has been learned from this effort, it has left unresolved the question of how this gut-brain communication is represented in the activity of specific neural circuits. Indeed, we know remarkably little about how any nutritional signal influences the dynamics of feeding circuits in an awake, behaving animal.

To observe this gut-brain communication directly, we developed a preparation that combines intragastric nutrient infusion with optical recording of AgRP neuron dynamics in awake, behaving mice. This preparation separates the hard-wired regulation of AgRP neurons by nutrients from their learned regulation by sensory cues. Using this approach, we have discovered layers of previously unsuspected regulation of these cells. We have found that AgRP neurons are inhibited by gastrointestinal nutrients on a timescale of minutes, in a way that is proportional to the number of calories infused but independent of macronutrient identity or nutritional state. We have further shown that this negative feedback loop involves a combination of gut hormones that are differentially required for the response to different nutrients. Conversely, we have shown that leptin, the most widely-studied hormone that regulates feeding, modulates circuit dynamics only on a timescale of hours. These findings reveal fundamental mechanisms that govern hunger and satiety, while also demonstrating a generally applicable strategy for dissecting gut-brain communication.

AgRP neurons are inhibited by gastrointestinal nutrients during satiation

Studies of the regulation of AgRP neurons have traditionally focused on a small set of hormones, including most prominently leptin and ghrelin (Cowley et al., 2001; Cowley et al., 2003; Nakazato et al., 2001; Pinto et al., 2004). While these hormones provide one mechanism for coupling AgRP neuron activity to nutritional state, their circulating levels are thought to reflect primarily long-term changes in energy balance, not acute fluctuations in nutrients caused by food consumption. Acute responses to food intake are instead mediated by gastric distension and the release of "gut peptides" which trigger satiation and meal termination (Cummings and Overduin, 2007). Satiation is predominantly a brainstem phenomenon (Grill and Norgren, 1978), which is modulated by but does not require input from the forebrain. Consequently it has remained unclear whether hypothalamic feeding circuits are informed of satiation in real-time and, if so, what signals are involved and what specific information is communicated.

We have shown here that AgRP neurons are inhibited by intragastric nutrients with kinetics that mirror the process of satiation, strongly suggesting that some of the same signals that govern meal termination regulate these cells. Consistent with this, we have demonstrated that three well-established satiation signals are sufficient to inhibit AgRP neuron activity *in vivo*: PYY, CCK, and 5HT. Interestingly, we have found that CCK is necessary for the inhibition of AgRP neurons by intragastric lipid, but dispensable for their regulation by

glucose (Figure 5), indicating that information about food intake is communicated to AgRP neurons in a nutrient-specific way. This implies that AgRP neurons are able to monitor the complex hormonal milieu that develops following consumption of different foods and extract information about their caloric content.

While CCK is necessary for the inhibition of AgRP neurons by intragastric lipid, the identity of the signals that are required for the response to intragastric protein and glucose remain unknown. We have shown that blood glucose levels do not correlate with AgRP neuron inhibition when glucose is delivered by different routes, indicating that circulating glucose is not the sole signal that communicates glucose ingestion to arcuate feeding circuits. We have also shown that GLP-1, the most prominent gastrointestinal peptide released following glucose ingestion, is not sufficient to inhibit AgRP neurons *in vivo*. However we cannot rule out more complex mechanisms involving interactions between glucose and hormones, nor can we exclude a role for intracellular glucose in regulating AgRP neuron activity directly (Andrews et al., 2008).

A second important question regards the pathway by which CCK and other signals communicate nutritional information to AgRP neurons *in vivo*. Receptors for CCK and PYY are expressed on vagal afferents that innervate the gastrointestinal tract (Berthoud, 2008), and abdominal vagotomy reduces the anorectic effect of both hormones (Koda et al., 2005; Reidelberger, 1994). Thus it is possible that these hormones communicate with AgRP neurons via an ascending neural pathway that includes vagal afferents. On the other hand, AgRP neurons express the PYY receptor (Broberger et al., 1997), and PYY can directly inhibit AgRP neuron firing in slice (Acuna-Goycolea and van den Pol, 2005), suggesting that circulating PYY may act directly on these cells. Combining the experimental preparation described here with systematic manipulation of the afferent pathways will enable these mechanisms to be distinguished

Leptin induces a slow modulation of AgRP and POMC neurons that is required for its ability to inhibit feeding

Leptin is a critical regulator of food intake thought to modulate its targets by two distinct mechanisms: gating of ion channels, resulting in rapid modulation of neural firing (Cowley et al., 2001; van den Top et al., 2004) and changes in gene expression, resulting in slower alterations in neural excitability (Pinto et al., 2004) and neurotransmitter levels (Schwartz et al., 1996; Stephens et al., 1995). While both of these mechanisms have been studied extensively using indirect and *ex vivo* approaches (Sohn et al., 2013), neither has yet been investigated by monitoring directly how leptin modulates the dynamics of feeding circuits *in vivo*.

To address this question, we measured how leptin administration modulates the activity of AgRP and POMC neurons in awake, behaving mice. To obtain a complete picture of this hormone's effects, we recorded calcium dynamics while systematically varying the leptin dose, route of delivery (injection versus infusion), timescale (minutes to days), genetic background (ob/ob versus wild-type), nutritional state (fasted versus fed) and measured readout (baseline activity versus sensory regulation). The unanimous finding from these experiments was that leptin has no acute effect on calcium dynamics in AgRP or POMC

neurons, but instead induces a slow modulation that develops over hours and persists as long as leptin is continually delivered. This change in baseline activity correlated with changes in food intake but surprisingly was neither necessary nor sufficient for the nutritional gating of the response of AgRP and POMC neurons to sensory cues. Complementary optogenetic manipulations demonstrated that AgRP neuron activation could bypass leptin's effects on feeding, suggesting that the slow inhibition of AgRP neurons is required for leptin's anorectic effects. Together, these findings reveal how leptin modulates its key neural targets *in vivo*.

In contrast to our findings, prior studies have reported rapid effects of leptin on AgRP and POMC neurons in slice (Claret et al., 2007; Cowley et al., 2001; Takahashi and Cone, 2005; van den Top et al., 2004). One possible explanation for this discrepancy is that fiber photometry measures population calcium dynamics and therefore may fail to detect changes in activity that occur in a small subset of cells. However the fact that we observe dramatic modulation of AgRP and POMC neurons in response to many other stimuli places an upper bound on the magnitude of any rapid leptin-mediated effect. Of note, this lack of a rapid response to leptin is consistent with the kinetics of the behavioral and autonomic responses to this hormone, which develop over hours (Pinto et al., 2004). Thus we propose that leptin's effects on feeding are mediated primarily by long-term changes in neural activity, probably involving transcription-dependent synaptic plasticity (Horvath, 2005; Horvath and Diano, 2004). This conclusion reemphasizes the importance of identifying the transcriptional targets of leptin, which remain poorly defined, in order to understand this hormone's biological effects.

AgRP neuron activity encodes an integrated estimate of energy balance

AgRP neurons are commonly described as "hunger neurons," but recent *in vivo* recording experiments have called into question what exactly is encoded in the activity of these cells (Betley et al., 2015; Chen et al., 2015; Mandelblat-Cerf et al., 2015). The rapid inhibition of AgRP neurons by the sight and smell of food suggests that they do not control hunger or food intake directly (Chen and Knight, 2016), although they powerfully modulate these processes by indirect means (Chen et al., 2016). In the present study, we have described how AgRP neurons are regulated by visceral signals, which has revealed previously unknown layers of interactions between nutrients, hormones, nutritional state, and sensory cues. How do these observations fit together to explain the biological function of these cells?

The data presented here demonstrate that AgRP neurons receive three streams of information, each of which evolves on a different timescale (Figure S7). The first stream consists of homeostatic signals, such as leptin, that report on energy reserves within the body and fluctuate over hours (Figure 6). The second stream consists of signals triggered by nutrient detection in the gut that report on calories ingested over the past few minutes (Figure 2). The third stream consists of sensory cues from the outside world that report on the moment-by-moment availability of food (Betley et al., 2015; Chen et al., 2015; Mandelblat-Cerf et al., 2015) and predict imminent food consumption (Figure 3 and S3). We propose that the function of AgRP neurons is to integrate these three streams of information to generate a coherent estimate of the animal's energy needs. Importantly, this process takes

into account not only current energy reserves, but also predicted changes in energy balance due to ongoing or impending food intake. Such an integration of feedforward and feedback signals would enable the most accurate estimate of energy balance, which would have obvious survival benefit. We believe that accumulating evidence supports this model of AgRP neurons as "energy calculators" that estimate nutritional state and then broadcast this information to downstream circuits, rather than as neurons that directly control a behaviorial output. An important challenge for the future will be to clarify further how AgRP neurons perform this energy calculation, since this is likely a major determinant of body weight in mammals.

Experimental Model and Subject Details

Experimental protocols were approved by the University of California, San Francisco IACUC following the National Institutes of Health guidelines for the Care and Use of Laboratory Animals. Animals were housed in 12-hour dark/light cycle with *ad libitum* access to food and water. Prior to experiments, animals were fasted for 16 hours as noted in the main text; they maintained *ad libitum* access to water. AgRP-IRES-Cre animals have been previously described and have been back-crossed onto a C57BL/6 background. To generate leptin-deficient AgRP-IRES-Cre (#012899) and POMC-Cre (#005965) mice, AgRP-IRES-Cre and POMC-Cre mice were crossed to ob/+ mice on a C57BL/6 background. Double heterozygous offspring were then crossed to generate AgRP-IRES-Cre or POMC-Cre mice on an ob/ob background with ob/+ littermates used as controls. For channelrhodopsin-2 expression in AGRP neurons, Agrp-IRES-Cre mice (#012899) were crossed with Ai32: ROSA26-loxStoplox-ChR2-eYFP (#012569) to generate double mutant animals. For channelrhodopsin-2 expression in AgRP neurons on a leptin deficient background, AgRP-IRES-Cre; ROSA- loxStoplox-ChR2-eYFP animals were crossed with AgRP-IRES-Cre;ob/+ mice. The offspring were then crossed to generate AgRP-IRES-Cre; ROSA- loxStoplox-ChR2-eYFP mice on an ob/ob background and ob/+ littermate controls. No statistical methods were used to determine sample sizes. Male and female mice ranging from 8-20 weeks were used. Animals used in intragastric infusion experiments were individually housed, and a cohort of 7 animals were used for experiments with nutrient infusion. A separate group of 4 animals was used for antagonist studeis. All other mice were group-housed.

Method Details

Stereotaxic surgery

For photometry experiments, we used recombinant AAV expressing cre-dependent GCaMP6s (AAV1.CAG.Flex.GCaMP6s, Penn Vector Core). AAV was stereotaxically injected unilaterally above the arcuate nucleus of AgRP-IRES-Cre, POMC-IRES-Cre, AgRP-IRES-Cre; ob/ob, AgRP-IRES-Cre; ob/+, POMC-IRES-Cre; ob/ob, and POMC-IRES-Cre; ob/+ mice. During the same surgery a commercially-available photometry cannula (Doric Lenses; MFC_400/430-0.48_6.1mm_MF2.5_FLT) or a custom-made photometry cannula (Thorlabs BFH48-400, F112, CF440-10; Chen et al., 2015) was implanted unilaterally in the ARC at the coordinates x=-0.3mm, y=-1.85mm, z=-5.8mm

from bregma for AgRP mice and x=-0.3, y=-1.75, z=-5.8 from bregma for POMC mice. For any given set of experiments the same kind of cannula was used. Mice were allowed 2–4 weeks for viral expression and recovery from surgery before photometry recording, mini-osmotic pump implantation or intragastric catheter implantation.

For optogenetic experiments, custom-made fiberoptic implants (Thorlabs ; 0.39 NA Ø200 mm core FT200UMT and CFLC230-10) were placed unilaterally above the arcuate nucleus of AgRP-IRES-Cre; ROSA-loxStoplox-ChR2-eYFP; ob/ob and AgRP-IRES-Cre; ROSA-loxStoplox-ChR2-eYFP; ob/+ mice at the coordinates x=-0.25 from bregma, y=-1.7 from bregma, z=-5.6 to -5.7 from dorsal skull surface. Mice were allowed 2–3 weeks recovery from surgery before behavior experiments or mini-osmotic pump implantation.

Intragastric catheter implantation

Intragastric catheters were made and implanted as described in detail previously (Ueno et al., 2012). Catheters were constructed by attaching 8cm of Silastic tubing (Silastic, Cat 508-003) and 8 cm Tygon tubing (Tygon, AAD04119) to opposite ends of a curved metal connector (Component Supply Company, NE-9019). A 1 cm circle of biologically compatible mesh (gifted by Raul Lazaro) was attached to the silastic tubing 2.3-2.8 cm distal to the edge of the metal connector using adhesive (Xiameter RTV-3110 base and Dow Corning 4 catalyst). A 1 cm by 1.5 cm oval of felt was affixed to the silastic tubing at the distal edge of the the curve in the connector and a 0.5 cm by 1 cm strip of felt was affixed around the metal connector on the proximal edge of its curve. A luer adapter was placed into the free end of the Tygon tubing (Instech, LS20). Assembled catheters were sterilized using ethylene oxide.

AgRP-IRES-Cre mice with functional photometry implants were anesthetized with ketamine/xylazine and the surgical areas shaved and scrubbed with betadine and alcohol. A skin incision of about 1 cm was made between the scapula and the skin dissected from the subcutaneous tissue toward the left flank. A midline abdominal skin incision about 1.5 cm was made extending from the xyphoid process caudally and the skin was dissected from the subcutaneous tissue toward the left flank to complete a subcutaneous tunnel between the two incisions. A hemostat was used to pull the sterilized catheter through the tunnel. The linea alba was incised and the abdominal cavity entered. A small incision was made in the left lateral abdominal wall through which the intragastric catheter was passed into the abdominal cavity. The stomach was externalized and a small puncture made using a jeweler's forcep. The tip of the cathether was immediately placed into the puncture site and sutured into place using the felt circle with polypropylene suture (CP Medical 8695P). Saline injection into catheter confirmed absence of leakage. The stomach was placed back in the abdominal cavity which was washed with sterile saline. The abdominal muscle was sutured and the skin incision closed in two layers. Next, the catheter was secured at its interscapular site with sutures into the felt oval and surrounding muscle. Finally, the interscapular skin incision was closed. Post-operatively, mice were treated with enrofloxacin, normal saline, and buprenorphine and allowed 7-10 days to recover prior to intragastric infusion and photometry experiments.

Mini-osmotic Pump Implantation

Mini-osmotic pumps with a release rate of about 0.5 uL/h (Alzet, Model 2002) were filled with vehicle or leptin to achieve release of 450 ng leptin per hour. These pumps were implanted subcutaneously into the dorsum of mice. An incision was made and a subcutaneous pocket created by tissue spreading. The pump was placed in this pocket and the skin wound closed with sutures.

Fiber photometry

Two rigs for performing fiber photometry recordings were constructed following basic specifications previously described with minor modifications (Chen et al., 2015; Gunaydin et al., 2014). A 473 nm laser diode (Omicron Luxx) was used as the excitation source. This was placed upstream of an optic chopper (Thorlabs MC2000) that was run at 400 Hz. Laser was then split with beam splitter (Thorlabs CM1-BS013). Split laser beams each bounced through two kinetic mirrors (Thorlabs BB1-E02, KM100) to allow adjustment of light path. Each laser beam was passed through a GFP excitation filter (Thorlabs MF469-35), reflected by a dichroic mirror (Semrock FF495-Di03-25x36) and coupled through a fiber collimation package (Thorlabs F240FC-A) into a home-made patchcord made with optical fiber (400 mm, 0.48 NA; Thorlabs BFH48-400) or a commercially available patchcord (Doric Lenses, MFP_400/430/1100-0.48_2m_FCM-MF2.5). Patchcords were not changed within experiments. The patchcords were then linked to a fiberoptic implants through ceramic (FIS F18300SSC25) or bronze (Doric Lenses, SLEEVE_BR_2.5) splitting sleeves. Fluorescence outputs were each filtered through a GFP emission filter (Thorlabs MF525-39) and focused by convex lenses (Thorlabs LA1255A) onto photoreceivers (Newport 2151). The signals were output into lock-in amplifiers (Stanford Research System, SR810) with time constant at 30 ms to allow filtering of noise at higher frequency. Those two lock-in amplifiers receive frequency signal of chopper split by BNC splitter. Signals were then digitized with a LabJack U6-Pro and recorded using software provided by LabJack (http://labjack.com/support/software) with 250 Hz sampling rate.

To reduce photobleaching during recordings that exceeded 3 hours, the laser was modulated as 1 second pulse every 10 seconds by a TTL signal generator (Graphic State software, Habitest H03-14). A copy of this TTL signal is also sent to LabJack U6-Pro. Each pulse was then extrapolated into a single data point by calculating the median of the center 50%. All experiments were performed in operant chambers (Coulbourn H10-11M-TC) inside a sound attenuating cubicle (Med Associates Inc ENV-022MD). Experiments were performed during the dark cycle in a dark environment. Mice that didn't show significant baseline calcium transient, ghrelin response or sensory response to peanutbutter or chow were assumed to be technical failures and were excluded from further experiments or further analysis.

To ensure consistent quality of data acquisition, we put the mating sleeve (FIS F18300SSC25) on the implanted cannula after surgery. The sleeve serves as a shield of implanted fiberoptic from scratches and also a gripping point for us to connect the mouse to the photometry rig with enough force to push fiberoptic ends together. Of note, we did not anesthetize the mice before connecting them to the photometry rig. To minimize contamination of the signal by dust in the light path, we cleaned the fiberoptic on the mouse

with connector cleaning sticks (MCC25) and precision fiber cleaning fluid (Thorlabs FCS3) or 70% ethanol before each recording. A syringe needle was used to pick out debris which occasionally became stuck in the sleeve. For comparison of data across different days, we let the mouse express virus for at least 6 weeks prior to experiments, which allows GCAMP expression to stabilize. We also refrained from re-aligning light path of photometry rig to ensure consistency.

Intragastric infusions

Nutrients at the indicated concentrations or water were infused via ingragastric catheters using a syringe pump (Harvard Apparatus, 70-2001). All infusions were delivered at 50 microliters per minute with a total infusion volume of 1.2 mL. All photometry experiments involving intragastric infusion were performed in fasted animals unless otherwise specified. Animals were habituated to behavioral chambers for 20 min during photometry recording. During this time, the intragastric catheter was attached to the syringe pump using plastic tubing and adapters (Tygon, AAD04119; Instech, LS20). Total infusion time was 24 min for all experiments. Photometry recording was continued for 15 min after the end of infusion before animals were presented with chow (PicoLab 5058) and then for 20 min following chow presentation. One to three trials of the same experiment for each mouse were combined, averaged, and treated as a single replicate. For peristimulus plots, time zero was defined as the moment that the infusion pump started.

All nutrients were diluted into deionized water fresh for each experiment. Vanilla Ensure powder was dissolved at a concentration of 0.42 g/mL of solution; 20% intralipid (Sigma-Aldrich) was used both undiluted and diluted to 6.4%; premium collagen peptides (Sports Research) was dissolved at concentrations of 0.45 g/mL and 0.15 g/mL; glucose was dissolved at 0.45 g/mL, 0.24 g/mL, 0.12 g/mL, and 0.06 g/mL; sucrose, fructose and galactose were dissolved at 0.24 g/mL; and sucralose was dissolved at 8 mg/mL.

Drug and hormone injections

Hormones and small molecules were injected at the concentrations and routes indicated below during photometry recording. All compounds were injected at a volume of 10 uL/g body weight. Animals were habituated to the recording chambers for 20 minutes prior to injection. Following hormone injection, photometry recording continued for 35 min or longer as indicated. For the combination injection of leptin and CCK, leptin was injected 2 hours prior to the start of recording, and then animals were habituated and injected with CCK as described for other experiments. For other hormone combinations, both hormones were injected simultaneously after habituation to the recording chamber. One to three trials of the same experiment for each mouse were combined, averaged, and treated as a single replicate. For peristimulus plots, time zero was defined as the moment that the investigator opened the behavioral chamber.

To evaluate the effect of LPS on feeding and on sensory inhibition of AgRP neurons, we presented LPS- or PBS-treated animals with chow 4 hours after injection (Essner et al., 2017). Fasted mice were injected with LPS or PBS 3.5 hours prior to placement in the recording chambers. After 30 min of recording animals were presented with chow (PicoLab

5058). Photometry recording continued for 20 min after chow presentation after which the quantity of chow consumed was measured. One trial each of LPS and PBS was performed per mouse in an LPS-naïve cohort

We used the following doses based on previously published reports, unless otherwise specified. Glucose 4.5 g/kg IP (Sigma), CCK octapeptide 10 ug/kg IP (Bachem), serotonin hydrochloride 2 mg/kg IP (Sigma-Aldrich), PYY 0.1 mg/kg IP (R&D Systems), leptin 2 mg/kg IP (R&D Systems), liraglutide 0.4 mg/kg IP (Novo Nordisk; generous gift from Dr. Randy Seeley), amylin 10 ug/kg IP (Tocris), glucagon 2 mg/kg SQ (Bachem), lithium chloride 84 mg/kg IP (Acros), LPS 100 ug/kg (Sigma), and ghrelin 2 mg/kg IP (R&D Systems). All of these compounds were dissolved in saline except for glucose which was dissolved in water.

Antagonist studies

To observe the effects of devazepide and ondansetron on baseline AgRP neuron activity, these antagonists or vehicle controls were injected via intragastric catheters into fasted mice after 20 min of habituation to the behavioral chamber during photometry recording. 3-5 min after drug injection, animals received intragastric infusion of water, which has no effect on AgRP neuron activity. AgRP neuron activity in antagonist-injected mice was compared to vehicle-injected controls (devazepide) or to animals who received only water infusion (ondansetron) at a time point 25 min after antagonist injection. To observe the effects of JNJ-31020028 on AgRP neuron activity, this drug was injected subcutaneously into fasted mice after 20 min of habituation to the behavioral chamber during photometry recording. This route was chosen because this drug is not orally bioavailable (Shoblock et al., 2010). Signal from these animals was compared to signal from vehicle-injected mice 25 min after injection. For peristimulus plots, time zero was defined as the moment that the investigator opened the behavioral chamber.

To observe the effects of antagonists on the response of AgRP neuron activity to nutrient infusion, animals were habituated to the recording chambers for 20 minutes prior to antagonist delivery. For devazepide and ondansetron, intragastric infusion of lipid, glucose, or water was started 3-5 min after antagonist delivery. For JNJ-31020028, intragastric infusion of lipid, glucose, or water infusion was started 25-30 minutes after antagonist delivery, since this is the time at which drug reaches maximum serum concentration (Shoblock et al., 2010). Infusion time was 24 min for all experiments. Photometry recording was continued for 15 min after infusion. For peristimulus plots time zero was defined as the moment that the infusion pump was started.

Doses were chosen based on previously published reports: devazepide 1 mg/kg IG (R&D Systems) was diluted in 5% DMSO, 5% Tween 80 in PBS, ondansetron 1 mg/kg IG (Sigma) was diluted in normal saline, and JNJ-31020028 10 mg/kg SC (MedKoo Biosciences) was diluted in 5% DMSO, 5% Tween 80 in PBS. All compounds were injected at a volume of 10 uL/g body weight.

Food and Object Presentation

To eliminate any effects of novelty, mice were exposed prior to testing to peanut butter, chocolate, and "cages" as described in the main text. Mice were either fasted overnight (16 h) or fed *ad libitum*, acclimated to the behavioral chamber, and then presented with chow, peanut butter, caged chocolate, or available chocolate as indicated in the main text. For peristimulus plots time zero was defined as the moment that the investigator opened the behavioral chamber.

Optogenetic Feeding Behavior

Optogenetic stimulation was performed as previously described. A 473 nm laser was modulated by Coulbourn Graphic State software through a TTL signal generator (Coulbourn H03-14) and synchronized with behavior experiments. The laser was split through a 4-way splitter (Fibersense and Signals) or passed through a single patch cable (Doric Lenses). The laser was then passed to custom-made fiber optic patch cables (Thorlabs FT200UMT, CFLC230-10; Fiber Instrument Sales F12774) through a rotary joint (Doric Lens FRJ 1×1). Patch cables were connected to the implants on mice through a zirconia mating sleeve (Thorlabs ADAL1). For opto-stimulation protocols, laser was modulated at 20 Hz on a 2 s ON and 3 s OFF cycle with 10 ms pulse width. Laser power was set between 15–20 mW at the terminal of patch cable. We estimated the light power at the ARC to be 4.02 mW/mm2. Effective power is likely lower due to loss at the cable-implant connection. Feeding behavior experiments were performed as previously described (Chen et al., 2015). Mice were allowed to recover for seven days after optogenetic implant surgery before experiments. Mice were habituated to the behavioral chambers (Coulbourn H10-11M-TC with H10-11M-TC-NSF), food pellets (20 mg Bio-Serv F0163) and pellet dispensing systems (Coulbourn H14-01M-SP04 and H14-23M) for three days before the first experiment.

All pre-stimulation food intake experiments follow this general structure: 70 min habituation/pre-stimulation period with no food access followed by 60 min food access. For prestimulation protocol, laser stimulation was on for the last 60 min of 70 min habituation/pre-stimulation period; for costimulation protocol, laser stimulation was on during the 60 min food access period. Pellet removal from the pellet dispensing system was detected using a built-in photo-sensor (Coulbourn H20-93). A pellet was dispensed roughly 10 seconds after each removal. Food pellets left on the ground after each session were counted and deducted from the total food consumed. Experiments were run during the early phase of the light cycle. Starting from habituation until the end of experiments, mice were given *ad libitum* access to the food pellets in additional to regular chow as food in their home cage.

Quantification and Statistical Analysis

Photometry analysis

Data were analyzed using a custom MatLab script. For intragastric infusion and IP hormone injection experiments, background fluorescence was corrected by subtracting the photometry signal in the absence of mice from total signal. Data were then low-pass filtered at 0.5 Hz due to their slow and sustained change in response to stimuli and down sampled to 10 Hz; data recorded with pulse laser (1 second per 10 seconds) were not processed with this step.

For peri-stimulus time plots, unless otherwise specified, the median value of data points in a 2 min window flanking the −5 min time point before each treatment was used as the normalization factor (F0) to calculate $\Delta F(t)/F0 = (F(t)-F0)/F0$. In Figure 3, F0 for the sensory response to chow following IG infusion was defined as the F0 prior to IG infusion. For experiments where recording data was sampled from pulsed lasers, the median of all data points 15 min before each treatment was used as the normalization factor to ensure reliable representation of the activity state. For experiments that track fluorescence signal strength across different days, the median of data points measured 20-30 min after the start of the photometry recording session on day 0 were used as the normalization factor (F0). The median of the fluorescent signal 20-30 min after the start of experiments on each of the subsequent days was defined as F(t) and used to estimate $\Delta F(t)/F0 = (F(t)-F0)/F0$.

For all experiments correction for photobleaching was not necessary due to the low laser power used during photometry recordings (~0.07 mW), the short time windows for most experiments (around 60 min), pulsed laser used for long-term experiments and the fact that all experimental groups had control groups treated with identical laser powers. In addition, correction for photobleaching could easily cause over-correction due to the slow and sustained effect in our experiments. To calculate the change of fluorescent signal at indicated time points after treatment, all data points F(t) over the indicated time range were averaged as Fa to estimate $\Delta Fa/F0 = (Fa-F0)/F0$.

Behavior Data Analysis

Data were analyzed using a custom MatLab script. Consumption of each pellet was defined as the first pellet removal event after each food pellet delivery. Total food consumption was estimated by subtracting the pellets found dropped after each experiment from the total number of food removal events. Multiple trials of the same experiment for each mouse were combined, averaged, and treated as a single replicate.

Statistical analysis

Fiber photometry data were subjected to analysis as described above. In Figures 1-5, 7, and S2-S5 ΔF/F(%) represents the mean $\Delta F(t)/F0*100$. Bar graphs depicting photometry data in these figures show the mean ΔF/F(%) over a 5 minute time window as indicated in the figure legends. For the 3h photometry recordings shown in figure 6 and figure S6, bar graphs depict the mean ΔF/F(%) over a 15-min window from 165-180 min after injection. For photometry signal comparisons across days shown in figure 6, ΔF/F(%) represents $\Delta F(t)/F0*100$ as described in photometry analysis.

The effects of different intragastric infusates, hormone injections, or receptor antagonists on fluorescence changes in photometry experiments as well as changes in blood glucose following intragastric infusion were analyzed using two-way, repeated-measures ANOVA. Changes in fluorescence in response to chow presentation and quantity of chow consumption after intragastric infusion were compared using one-way ANOVA. The effects of leptin administration and presentation of food in leptin-deficient and control mice on fluorescence changes in photometry experiments as well as changes in food intake following mini-osmotic pump delivery of leptin were analyzed using two-way ANOVA. The effects of

optogenetic stimulation on food intake were compared using two-way, repeated-measures ANOVA. The Holm-Sidak multiple comparisons test was used in conjunction with ANOVA. All statistical analysis was performed using Prism. Numbers of animals are included in the figure legends. Significance was defined as $P < 0.05$ and is indicated on figures and in figure legends.

Supplementary Material

Refer to Web version on PubMed Central for supplementary material.

Acknowledgments

References

Acuna-Goycolea C, van den Pol AN. Peptide YY3-36 inhibits both anorexigenic proopiomelanocortin and orexigenic neuropeptide Y neurons: Implications for hypothalamic regulation of energy homeostasis. Journal of Neuroscience. 2005; 25:10510–10519. [PubMed: 16280589]

Andermann ML, Lowell BB. Toward a Wiring Diagram Understanding of Appetite Control. Neuron. 2017; 95:757–778. [PubMed: 28817798]

Andrews ZB, Liu ZW, Walllingford N, Erion DM, Borok E, Friedman JM, Tschop MH, Shanabrough M, Cline G, Shulman GI, et al. UCP2 mediates ghrelin's action on NPY/AgRP neurons by lowering free radicals. Nature. 2008; 454:846–851. [PubMed: 18668043]

Barrachina MD, Martinez V, Wang LX, Wei JY, Tache Y. Synergistic interaction between leptin and cholecystokinin to reduce short-term food intake in lean mice. Proceedings of the National Academy of Sciences of the United States of America. 1997; 94:10455–10460. [PubMed: 9294232]

Becskei C, Lutz TA, Riediger T. Glucose reverses fasting-induced activation in the arcuate nucleus of mice. Neuroreport. 2008; 19:105–109. [PubMed: 18281902]

Berthoud HR. The vagus nerve, food intake and obesity. Regulatory peptides. 2008; 149:15–25. [PubMed: 18482776]

Betley JN, Xu S, Cao ZF, Gong R, Magnus CJ, Yu Y, Sternson SM. Neurons for hunger and thirst transmit a negative-valence teaching signal. Nature. 2015; 521:180–185. [PubMed: 25915020]

Broberger C, Landry M, Wong H, Walsh JN, Hokfelt T. Subtypes Y1 and Y2 of the neuropeptide Y receptor are respectively expressed in pro-opiomelanocortin- and neuropeptide-Y-containing neurons of the rat hypothalamic arcuate nucleus. Neuroendocrinology. 1997; 66:393–408. [PubMed: 9430445]

Chen Y, Knight ZA. Making sense of the sensory regulation of hunger neurons. BioEssays : news and reviews in molecular, cellular and developmental biology. 2016; 38:316–324.

Chen Y, Lin YC, Kuo TW, Knight ZA. Sensory detection of food rapidly modulates arcuate feeding circuits. Cell. 2015; 160:829–841. [PubMed: 25703096]

Chen Y, Lin YC, Zimmerman CA, Essner RA, Knight ZA. Hunger neurons drive feeding through a sustained, positive reinforcement signal. eLife. 2016:5.

Claret M, Smith MA, Batterham RL, Selman C, Choudhury AI, Fryer LG, Clements M, Al-Qassab H, Heffron H, Xu AW, et al. AMPK is essential for energy homeostasis regulation and glucose sensing by POMC and AgRP neurons. The Journal of clinical investigation. 2007; 117:2325–2336. [PubMed: 17671657]

Clemmensen C, Muller TD, Woods SC, Berthoud HR, Seeley RJ, Tschop MH. Gut-Brain Cross-Talk in Metabolic Control. Cell. 2017; 168:758–774. [PubMed: 28235194]

Cowley MA, Smart JL, Rubinstein M, Cerdan MG, Diano S, Horvath TL, Cone RD, Low MJ. Leptin activates anorexigenic POMC neurons through a neural network in the arcuate nucleus. Nature. 2001; 411:480–484. [PubMed: 11373681]

Cowley MA, Smith RG, Diano S, Tschop M, Pronchuk N, Grove KL, Strasburger CJ, Bidlingmaier M, Esterman M, Heiman ML, et al. The distribution and mechanism of action of ghrelin in the CNS demonstrates a novel hypothalamic circuit regulating energy homeostasis. Neuron. 2003; 37:649–661. [PubMed: 12597862]

Cummings DE, Overduin J. Gastrointestinal regulation of food intake. Journal of Clinical Investigation. 2007; 117:13–23. [PubMed: 17200702]

Essner RA, Smith AG, Jamnik AA, Ryba AR, Trutner ZD, Carter ME. AgRP neurons can increase food intake during conditions of appetite suppression and inhibit anorexigenic parabrachial neurons. The Journal of neuroscience : the official journal of the Society for Neuroscience. 2017

Grill HJ, Norgren R. Chronically decerebrate rats demonstrate satiation but not bait shyness. Science. 1978; 201:267–269. [PubMed: 663655]

Gunaydin LA, Grosenick L, Finkelstein JC, Kauvar IV, Fenno LE, Adhikari A, Lammel S, Mirzabekov JJ, Airan RD, Zalocusky KA, et al. Natural neural projection dynamics underlying social behavior. Cell. 2014; 157:1535–1551. [PubMed: 24949967]

Horvath TL. The hardship of obesity: a soft-wired hypothalamus. Nature neuroscience. 2005; 8:561–565. [PubMed: 15856063]

Horvath TL, Diano S. The floating blueprint of hypothalamic feeding circuits. Nature reviews Neuroscience. 2004; 5:662–667. [PubMed: 15263896]

Koda S, Date Y, Murakami N, Shimbara T, Hanada T, Toshinai K, Niijima A, Furuya M, Inomata N, Osuye K, Nakazato M. The role of the vagal nerve in peripheral PYY3-36-induced feeding reduction in rats. Endocrinology. 2005; 146:2369–2375. [PubMed: 15718279]

Mandelblat-Cerf Y, Ramesh RN, Burgess CR, Patella P, Yang Z, Lowell BB, Andermann ML. Arcuate hypothalamic AgRP and putative POMC neurons show opposite changes in spiking across multiple timescales. eLife. 2015:4.

Myers MG, Munzberg H, Leinninger GM, Leshan RL. The Geometry of Leptin Action in the Brain: More Complicated Than a Simple ARC. Cell metabolism. 2009; 9:117–123. [PubMed: 19187770]

Nakazato M, Murakami N, Date Y, Kojima M, Matsuo H, Kangawa K, Matsukura S. A role for ghrelin in the central regulation of feeding. Nature. 2001; 409:194–198. [PubMed: 11196643]

Pinto S, Roseberry AG, Liu H, Diano S, Shanabrough M, Cai X, Friedman JM, Horvath TL. Rapid rewiring of arcuate nucleus feeding circuits by leptin. Science. 2004; 304:110–115. [PubMed: 15064421]

Reidelberger RD. Cholecystokinin and control of food intake. The Journal of nutrition. 1994; 124:1327S–1333S. [PubMed: 8064379]

Richter CP. Total self-regulatory functions in animals and human beings. Harvey Lecture Series. 1942; 38:63–103.

Riediger T, Bothe C, Becskei C, Lutz TA. Peptide YY directly inhibits ghrelin-activated neurons of the arcuate nucleus and reverses fasting-induced c-Fos expression. Neuroendocrinology. 2004; 79:317–326. [PubMed: 15256809]

Schwartz MW, Baskin DG, Bukowski TR, Kuijper JL, Foster D, Lasser G, Prunkard DE, Porte D, Woods SC, Seeley RJ, Weigle DS. Specificity of leptin action on elevated blood glucose levels and hypothalamic neuropeptide Y gene expression in ob/ob mice. Diabetes. 1996; 45:531–535. [PubMed: 8603777]

Shoblock JR, Welty N, Nepomuceno D, Lord B, Aluisio L, Fraser I, Motley ST, Sutton SW, Morton K, Galici R, et al. In vitro and in vivo characterization of JNJ-31020028 (N-(4-{4-[2-(diethylamino)-2-oxo-1-phenylethyl]piperazin-1-yl}-3-fluorophenyl)-2- pyridin-3-ylbenzamide), a selective brain penetrant small molecule antagonist of the neuropeptide Y Y(2) receptor. Psychopharmacology. 2010; 208:265–277. [PubMed: 19953226]

Sohn JW, Elmquist JK, Williams KW. Neuronal circuits that regulate feeding behavior and metabolism. Trends in neurosciences. 2013; 36:504–512. [PubMed: 23790727]

Stephens TW, Basinski M, Bristow PK, Buevalleskey JM, Burgett SG, Craft L, Hale J, Hoffmann J, Hsiung HM, Kriauciunas A, et al. The Role of Neuropeptide-Y in the Antiobesity Action of the Obese Gene-Product. Nature. 1995; 377:530–532. [PubMed: 7566151]

Takahashi KA, Cone RD. Fasting induces a large, leptin-dependent increase in the intrinsic action potential frequency of orexigenic arcuate nucleus neuropeptide Y/Agouti-related protein neurons. Endocrinology. 2005; 146:1043–1047. [PubMed: 15591135]

Tellez LA, Medina S, Han WF, Ferreira JG, Licona-Limon P, Ren XY, Lam TT, Schwartz GJ, de Araujo IE. A Gut Lipid Messenger Links Excess Dietary Fat to Dopamine Deficiency. Science. 2013; 341:800–802. [PubMed: 23950538]

Tolhurst G, Reimann F, Gribble FM. Intestinal sensing of nutrients. Handbook of experimental pharmacology. 2012:309–335. [PubMed: 22249821]

Ueno A, Lazaro R, Wang PY, Higashiyama R, Machida K, Tsukamoto H. Mouse intragastric infusion (iG) model. Nature protocols. 2012; 7:771–781. [PubMed: 22461066]

van den Top M, Lee K, Whyment AD, Blanks AM, Spanswick D. Orexigen-sensitive NPY/AgRP pacemaker neurons in the hypothalamic arcuate nucleus. Nature neuroscience. 2004; 7:493–494. [PubMed: 15097991]

Zimmerman CA, Lin YC, Leib DE, Guo L, Huey EL, Daly GE, Chen Y, Knight ZA. Thirst neurons anticipate the homeostatic consequences of eating and drinking. Nature. 2016

Highlights

Intragastric nutrients rapidly and durably inhibit hunger-promoting AgRP neurons

AgRP neuron inhibition by nutrients depends on total calories, not nutrient identity

A hormone screen identifies CCK, PYY, and 5HT as post-prandial AgRP neuron regulators

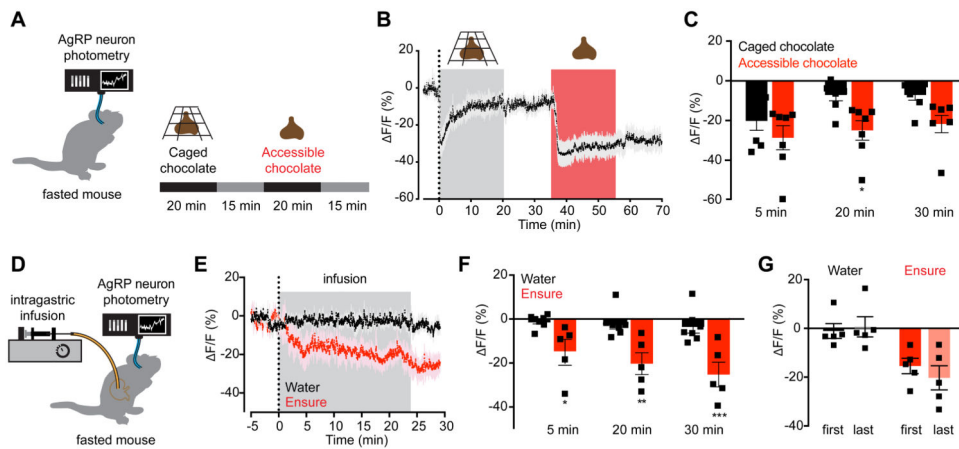Leptin induces slow modulation of AgRP and POMC neurons on a timescale of hours

Figure 1. Nutrient intake is necessary and sufficient for sustained AgRP neuron inhibition

(A) Schematic of experiment in (B-C). Fasted mice were presented with caged chocolate and then available chocolate during photometry recording from AgRP neurons.

(B) Calcium signal from AgRP neurons in fasted mice presented first with caged chocolate (gray) and then available chocolate (red) (n=7 mice).

(C) Quantification of ∆F/F from (B). Times shown are 5-min windows immediately after chocolate presentation (5 min), immediately prior to chocolate removal (20 min), and 10 min following chocolate removal (30 min). * P = 0.02 compared to caged chocolate (Holm-Sidak's multiple comparisons test adjusted p-value)

(D) Schematic of the experimental set-up for AgRP photometry recording during intragastric nutrient infusion for 24 min.

(E) Calcium signal from AgRP neurons in fasted mice during intragastric infusion with water (black) or Ensure liquid diet (red). Gray denotes infusion (n = 7 mice for water; n = 5 mice for Ensure).

(F) Quantification of ∆F/F from (E). Times shown are 5-min windows from the early part of infusion (5 min), the end of infusion (20 min), and 10 min following the end of infusion (30 min). *P< 0.05, **P = <0.01, ***P< 10-3 compared to water infusion at the indicated time point (Holm-Sidak's multiple comparisons test, adjusted p-value).

(G) Quantification of ∆F/F at the end of infusion following the first and last intragastric exposures to water (black) and Ensure (red). Infusions were separated by approximately 7 weeks.

(B and E) Traces represent mean ± SEM

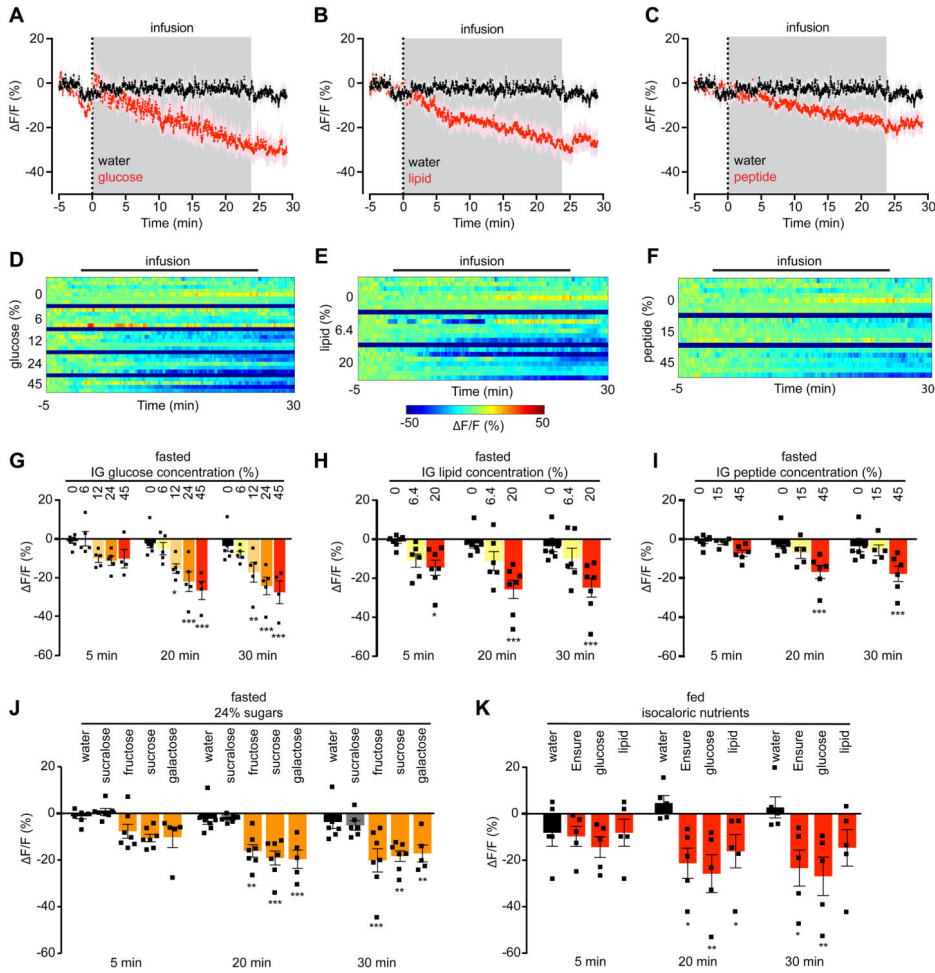(C,F,G) ■ denotes individual mice. Bars represent mean ± SEM

See also Figure S1.

Figure 2. Inhibition of AgRP neurons by nutrients is independent of macronutrient composition or nutritional state and is proportional to calorie ingestion

(A-C) Calcium signal from AgRP neurons in fasted mice during intragastric infusion with water (black) or isocaloric and isovolemic quantities of 45% glucose (A), 20% lipid (B), or 45% peptide (C) solutions (red). Traces represent mean ± SEM. Gray denotes infusion. (n = 4-7 mice per group)

(D-F) Peri-infusion heat maps depicting ΔF/F during photometry recording in fasted mice receiving intragastric infusion of the indicated concentrations of glucose (D), lipid (E), or peptide (F). Each row represents the average of 1-3 trials of an individual mouse. (n = 4-7 mice per group).

(G-I) Quantification of ΔF/F from (D-F).

(J) Quantification of ΔF/F during photometry recording in fasted mice receiving intragastric infusion of the indicated 24% mono- and disaccharide solutions or the non-caloric sweetener sucralose.

(K) Quantification of ΔF/F during photometry recording from AgRP neurons in *ad libitum* fed mice receiving intragastric infusion of the indicated isocaloric solutions. (n = 5 mice per group).

(G-K) ■ denotes individual mice. Times shown are 5-min windows from the early part of infusion (5 min), the end of infusion (20 min), and 10 min following the end of infusion (30

min). Bars represent mean ± SEM. *$P < 0.05$, **$P < 0.01$, ***$P < 10^{-3}$ compared to H_2O infusion at the indicated time point (Holm-Sidak multiple comparisons test, adjusted p-value).
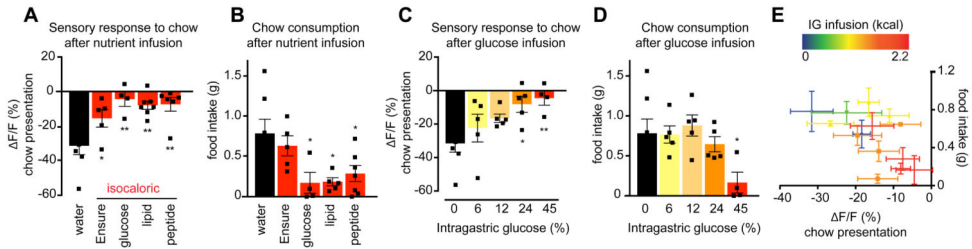
See also Figure S2.

Figure 3. AgRP neuron inhibition in response to the sensory detection of food is inversely related to intragastric calorie infusion and predicts subsequent chow consumption

(A and C) Quantification of ΔF/F during photometry recording from AgRP neurons in fasted mice for 5 min following chow presentation. Chow was presented 15 min after the end of intragastric infusion of the indicated nutrients. (n = 4-7 mice per group).

(B and D) Food intake was recorded for the first 20 minutes of re-feeding during the experiment described in (A and C).

(E) Correlation of ΔF/F following chow presentation with food intake during the first 20 minutes of re-feeding for all intragastric infusions in fasted animals shown in Figure 2. Points on the scatter plot represent mean ± SEM. Color gradient represents caloric content of the infusates.

(A-D) ■ denotes individual mice. Bars represent mean ± SEM. *$P < 0.05$, **$P < 0.01$ compared to H_2O infusion (Holm-Sidak multiple comparisons test, adjusted p-value). See also Figure S3.
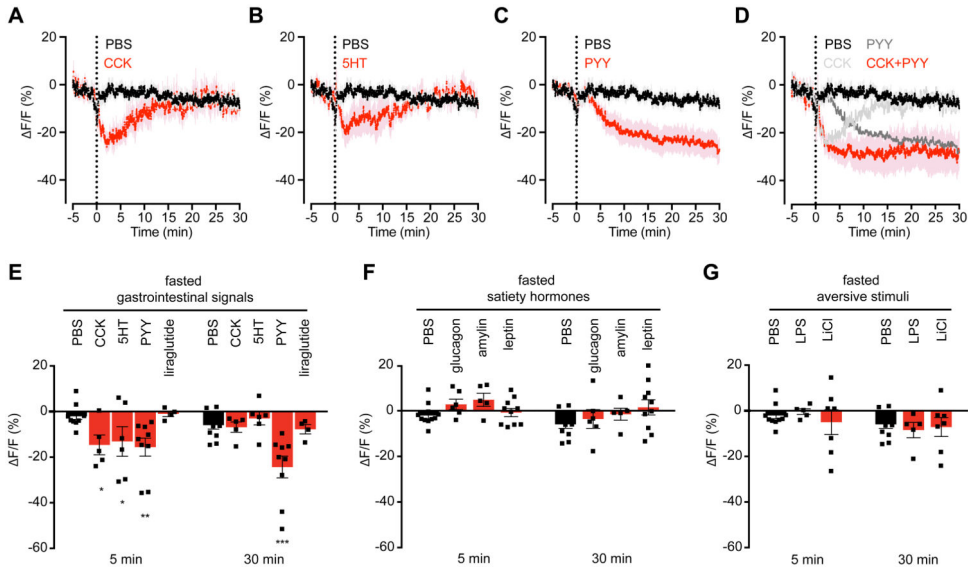
Figure 4. CCK, PYY, and 5HT are sufficient to inhibit AgRP neuron activity

(A-D) Calcium signal from AgRP neurons in fasted mice after IP injection with PBS (black) or CCK (A), 5HT (B), PYY(C), or a combination of CCK and PYY (D) (red). Traces represent mean ± SEM. Traces showing ΔF/F for individual injections of CCK and PYY are also shown in (D) (gray). (n=5-11 mice per group).

(E) Quantification of ΔF/F from (A-C). Quantification of ΔF/F following liraglutide injection is also shown.

(F and G) Quantification of ΔF/F during photometry recording in fasted mice following IP injection of the indicated compounds.

(E-G) ■ denotes individual mice. Times shown are 5-min windows 5 and 30 min after injection. Bars represent mean ± SEM. $*P < 0.05$, $**P < 0.01$, $***P < 10^{-3}$ compared to PBS injection at the indicated time point (Holm-Sidak multiple comparisons test, adjusted p-value).
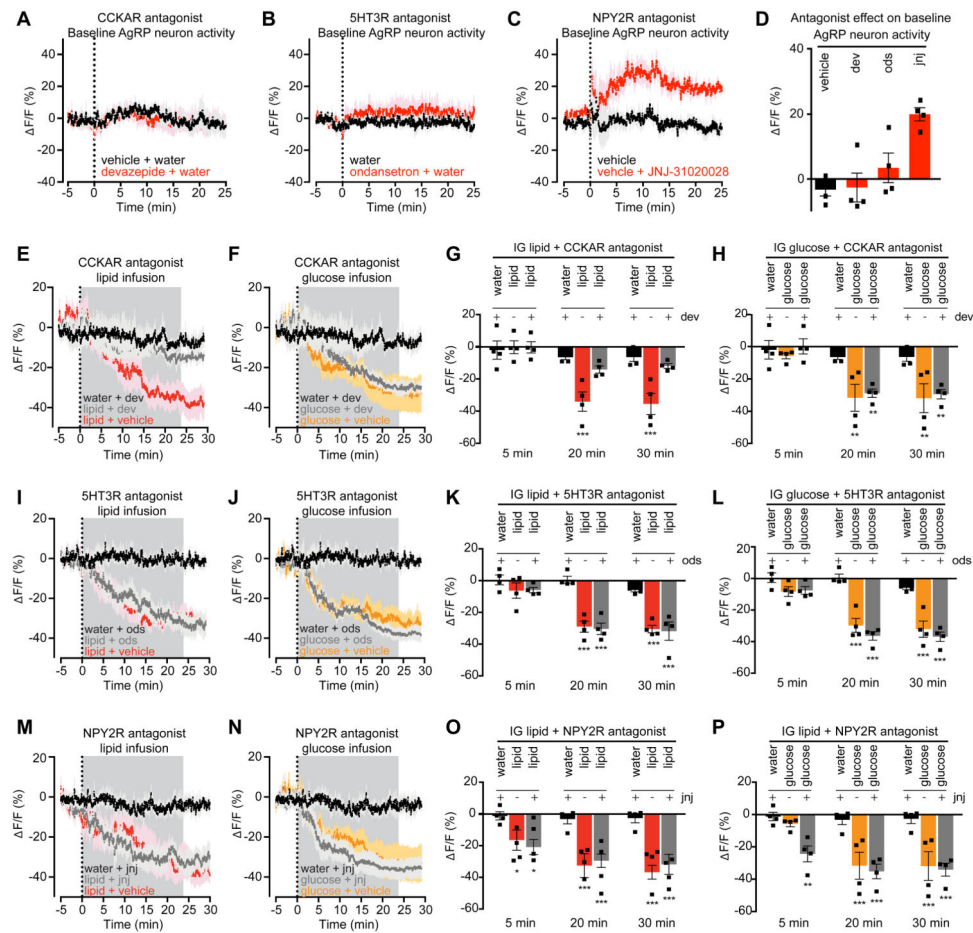
See also Figure S4.

Figure 5. PYY is necessary for inhibiting the basal firing rate of AgRP neurons. CCK is necessary for AgRP neuron inhibition caused by lipid

(A-C) Calcium signal from AgRP neurons in fasted mice in response to vehicle (black) or devazepide (dev, A), ondansetron (ods, B), or JNJ-31020028 (jnj, C) (red).

(D) Quantification of ΔF/F from (A-C). Time shown is a 5-min time window 25 min after antagonist administration.

(E and F) Calcium signal in fasted mice after intragastric injection of dev or vehicle followed by intragastric infusion of lipid (E) or glucose (F).

(G and H) Quantification of of ΔF/F from (E and F). n = 4 mice per group.

(I and J) Calcium signal from AgRP neurons in fasted mice after intragastric injection of ods or vehicle followed by intragastric infusion of lipid (I) or glucose (J).

(K and L) Quantification of of ΔF/F from (I and J). n = 4 mice per group.

(M and N) Calcium signal from AgRP neurons in fasted mice after subcutaneous injection of jnj or vehicle followed by intragastric infusion of lipid (M) or glucose (N).

(O and P) Quantification of of ΔF/F from (M and N). n = 4 mice per group.

(A-C, E, F, I, J, M, N) traces represent mean ± SEM

(G, H, K, L, O, P) Times shown are 5-min windows from the early part of infusion (5 min), the end of infusion (20 min), and 10 min following the end of infusion (30 min).

■ denotes individual mice. Bars represent mean ± SEM. $*P < 0.05$, $***P < 10^{-3}$ compared to vehicle at the indicated time point.
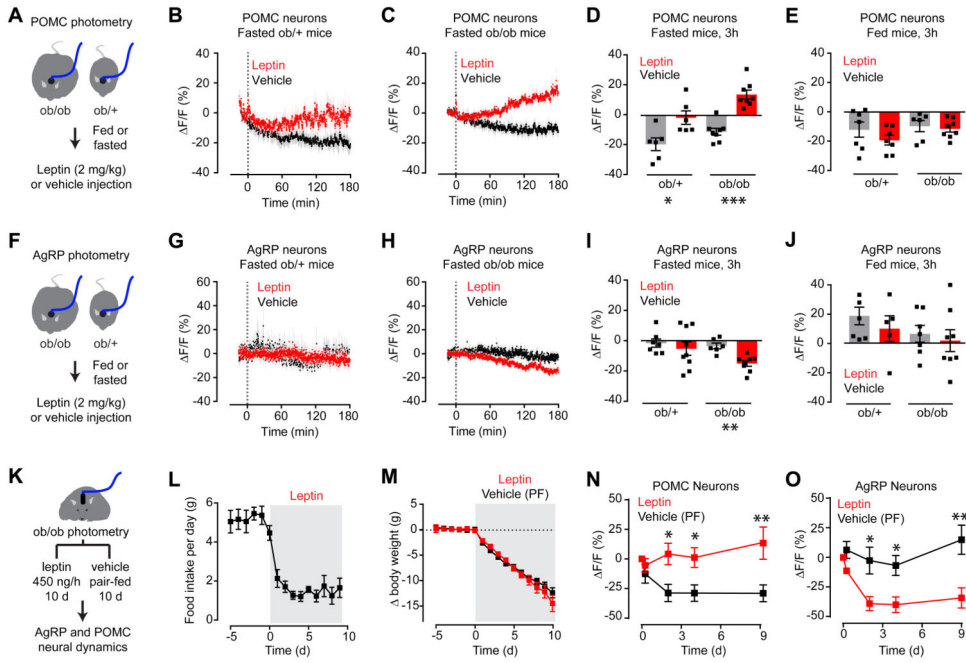
Figure 6. Leptin gradually modulates the activity of AgRP and POMC neurons in fasted animals

(A) Schematic of experiments in (B-E). 3 hour photometry recording from POMC neurons in fasted or fed ob/ob and ob/+ mice injected with leptin.

(B and C) Calcium signal from POMC neurons in fasted ob/+ (B) and ob/ob (C) mice after vehicle (black) or leptin (red) injection. (n = 6-8 mice per group).

(D and E) Quantification of ΔF/F of POMC neurons after prolonged photometry recording following IP injection of vehicle or leptin in fasted (D) and fed (E) states.

(F) Schematic of experiments in (G-J). 3 hour photometry recording from AgRP neurons in fasted or fed ob/ob and ob/+ mice injected with leptin.

(G and H) Calcium signal from AgRP neurons in fasted ob/+ (G) and ob/ob (H) mice after vehicle (black) or leptin (red) injection. (n = 7-8 mice per group)

(I and J) Quantification of ΔF/F of AgRP neurons after prolonged photometry recording following IP injection of vehicle or leptin in fasted (I) and fed (J) states.

(K) Schematic of experiments in (L-O). Body weight, food intake, and photometry signals from AgRP and POMC neurons were measured in ob/ob mice during chronic leptin or vehicle infusion by mini-osmotic pumps. Vehicle treated animals were pair-fed (PF) to leptin treated animals. Mini-osmotic pump was implanted at day 0

(L and M) Food intake (L) and change in body weight (M) following vehicle or leptin infusion. (n = 9 mice per group).

(N and O) Quantification of ΔF/F following vehicle (black) or leptin (red) infusion by mini-osmotic pump in POMC (N) and AgRP (O) neurons. (n = 4 mice).

(B, C, G, H, L, M, N, O) Traces represent mean ± SEM

(D,E,I,J) ■ denotes individual mice. Bars represent mean ΔF/F ± SEM over a 15-min window 3 hours after injection.

*$P < 0.05$, **$P < 0.01$, ***$P < 10^{-3}$
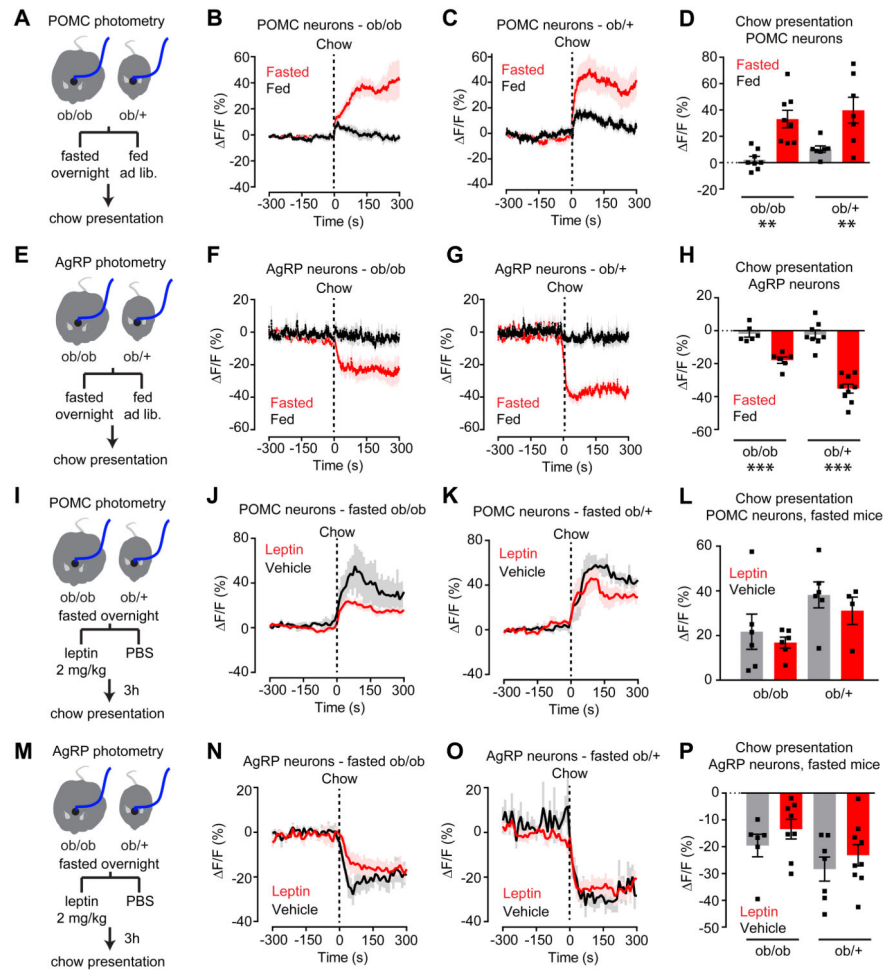
See also Figure S5.

Figure 7. Leptin is neither necessary nor sufficient for gating the sensory regulation of AgRP and POMC neurons

(A) Schematic of experiments in (B-D). Photometry recording from POMC neurons in fasted and fed ob/ob and ob/+ mice in response to chow presentation.

(B and C) Calcium signal from POMC neurons in ob/ob (B) and ob/+ (C) mice in response to chow presentation in the fed (black) or fasted (red) state. (n = 7-8 mice per group).

(D) Quantification of F/F from (B, C).

(E) Schematic of experiments in (F-H). Photometry recording from AgRP neurons in fasted and fed ob/ob and ob/+ mice in response to chow presentation

(F and G) Calcium signal from AgRP neurons in ob/ob (F) and ob/+ (G) mice in response to chow presentation in the fed (black) or fasted (red) state (n = 6-9 mice per group).

(H) Quantification of F/F from (F, G).

(I) Schematic of experiments in (J-L). Photometry recording from POMC neurons in fasted ob/ob and ob/+ mice in response to chow presentation after vehicle or leptin injection.

(J and K) Calcium signal from POMC neurons in ob/ob (J) and ob/+ (K) mice in response to chow presentation after vehicle (black) or leptin (red) injection. (n = 4-6 mice per group).

(L) Quantification of F/F from (J, K).

(M) Schematic of experiments in (N-P). Photometry recording from AgRP neurons in fasted ob/ob and ob/+ mice in response to chow presentation after vehicle or leptin injection.

(N and O) Calcium signal from AgRP neurons in ob/ob (N) and ob/+ (O) mice in response to chow presentation after vehicle (black) or leptin (red) injection (n= 6-9 mice per group).

(P) Quantification of F/F from (N,O).

(B, C, F, G, J, K, N, O) Traces represent mean ± SEM

(D,H,L,P) ■ denotes individual mice. Bars represent mean F/F ± SEM over a 5-min window following chow presentation. *$P < 0.05$, **$P < 0.01$, ***$P < 10^{-3}$
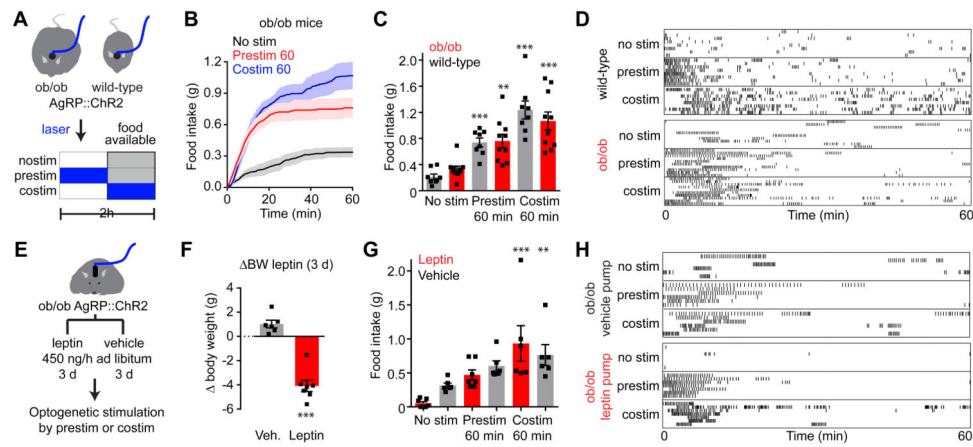
See also Figure S6.

Figure 8. AgRP neurons are epistatic to leptin's effect on food intake

(A) Schematic of experiments in (B-D). Optogenetic stimulation of AgRP neurons in *ad libitum* fed WT and ob/ob mice prior to (prestim) or during (costim) food availability. Blue indicates the timing of laser stimulation.

(B) Cumulative food intake by ob/ob mice after no stimulation (black), 60 min pre-stimulation (red), or during 60 min co-stimulation (blue). Traces represent mean ± SEM (n = 6-10 mice per group).

(C) Quantification of food intake from (B).

(D) Raster plots showing feeding pattern in individual mice from (B and C).

(E) Schematic of experiments in (F-H). Optogenetic stimulation of AgRP neurons in *ad libitum* fed, ob/ob mice during chronic vehicle or leptin infusion by mini-osmotic pumps. Stimulation occurred prior to (prestim) or during (costim) food availability as in (A).

(F) Bodyweight change in ob/ob mice 3 days after implantation of a mini-osmotic pump infusing vehicle (gray, n = 6 mice) or leptin (red, n = 7 mice)

(G) Quantification of food intake by *ad libitum* fed ob/ob mice from (F) receiving chronic vehicle (gray) or leptin (red) infusion after no stimulation, 60 min pre-stimulation, or during 60 min co-stimulation.

(H) Raster plots showing feeding pattern in individual mice from (G).

(C, F, G) ■ denotes individual mice. Bars represent mean ± SEM. *$P < 0.05$, **$P < 0.01$, ***$P < 10^{-3}$. (D and H) Each row represents a single trial from a different animal and each point indicates consumption of a 0.02 g pellet.

See also Figure S7.